Proc. IMECHE- Part E: Journal of Process Mechanical Engineering

https://uk.sagepub.com/en-gb/eur/proceedings-of-the-institution-of-mechanical-engineers-part-e-journal-of-process-mechanical

Accepted May 13th, 2024

Numerical study of electroconductive non-Newtonian hybrid nanofluid flow from a stretching rotating disk with a Cattaneo-Christov heat flux model

MD. Shamshuddin[1*], S.O. Salawu[2], O. Anwar Bég[3], Usman[4], Tasveer A. Bég[5] and S. Kuharat[3]

[1] *Department of Computer Science and Artificial Intelligence (Mathematics), SR University, Warangal-506371, Telangana,* ***India****.*

Emails: *shammaths@gmail.com; md.shamshuddin@sru.edu.in*

[2]*Department of Mathematics, Bowen University, Iwo,* ***Nigeria.***

Email: *kunlesalawu2@gmail.com*

[3]*Multi-physical Engineering Sciences Group (MPESG), Corrosion Lab, 3-08, SEE Bldg, Mechanical Engineering Department, Salford University, Manchester M54WT,* ***UK****.*

Email: *O.A.Beg@salford.ac.uk*

[4]*Department of Computer Science, National University of Sciences and Technology, Balochistan Campus (NBC), Quetta, 87300,* ***Pakistan****.*

Email: usman.malik.ms@gmail.com

[5]*Engineering Mechanics Research, Israfil House, Dickenson Rd., Longsight, Manchester, M13,* ***UK.***

Email: *tasveerabeg@gmail.com*

[3]*Multi-physical Engineering Sciences Group (MPESG), Corrosion Lab, 3-08, SEE Bldg, Mechanical Engineering Department, Salford University, Manchester M54WT,* ***UK****.*

Email: *S.Kuharat2@salford.ac.uk*

[*]*Corresponding author: shammaths@gmail.com, md.shamshuddin@sru.edu.in*

Orchid Number: 0000-0002-2453-8492

Abstract

Motivated by emerging technologies in smart functional nano-polymeric coating systems in pharmaceutical and robotics applications, the convective heat transfer characteristics in swirl coating with a magnetic hybrid power-law rheological nanofluid polymer on a radially stretching rotating disk are examined theoretically. An axial magnetic field is imposed. Copper (Cu**)** and Aluminium alloys (AA7075**)** nanoparticles with Sodium Alginate ($C_6H_9Na0_7$) as base fluid are considered, and a hybrid volume fraction model is deployed. A non-Fourier (Cattaneo-Christov) heat flux model is deployed to inspire thermal relaxation impacts absent in the classical Fourier heat conduction formulation. Through similarity proxies and the Von Karman transformations, the partial derivative systems of equations with associated boundary constraints are reduced to a system of derivative boundary value problems, which is solved numerically via the weighted residual method (WRM) with an integral Galerkin scheme, executed in the MAPLE symbolic software. Validation with special cases from articles is

captured. The computations revealed that radial, tangential and axial velocity are depleted, whereas temperature is enhanced with increasing magnetic parameter (*M*). High thermal transfers are obtained for the hybrid nanofluid relative to the AA7075 alloy nanofluid. A strong increment in temperature is also produced with a greater thermal relaxation effect.

Keywords: *Functional nanopolymers; coatings; Copper (Cu)/Aluminium alloy (AA7075) nanoparticles, weighted residual method (WRM), Galerkin scheme, power-law non-Newtonian model;*

1. Introduction

A strong trend in recent years in materials science and manufacturing technology has been the development and implementation of *magnetic nano-polymers*. These complex fluids combine polymer-like structures with magnetic nanoparticles (MNPs), achieving magneto-responsive, soft matter fluidic systems. These provide significant benefits in enhanced durability, formability, and anti-corrosion abilities by providing functional characteristics which can be manipulated via an intensity dynamical regulator with magnetic fields. Many different magnetic nano-polymers have been fabricated, including branching hybrids [1], ferromagnetic filaments (MFs) embedded in gel nanofluids [2], ferrite nanochain polymers [3], etc. These materials are finding increasing applications in advanced coatings, for example, supercapacitor applications [4]. A popular methodology in synthesising complex nano-coatings is using a rotating disk cathode [5]. Including rotation with MHD provides another mechanism for carefully controlling coating thickness and constitution of magnetic nanomaterials. It has been deployed in many cases in recent years, including Ni/diamond electromagnetic coatings [6], iron-silicon hybrid coatings [7], Cobalt-Iron coatings [8], plasma spraying in NiCrBSi electroconductive coatings [9] and pulsed MHD finishing for Nickel-Tungsten-Carbon composite nano-coatings [10].

The spin coating technique on a disk is gaining popularity in magnetic nanomaterials production. This invokes the dynamics of swirl flow. Historically, the great engineering scientist Von Karman addressed the Newtonian streaming fluid along a rotating disk surface theoretically [11]. Significant contributions were made by Cochran [12] on transient swirling flow. Later Sparrow and Cess [13] formulated the magnetohydrodynamic version of Von Karman's problem and included heat transfer. They noted that a stronger axial magnetic field suppresses all flow velocity components but enhances the torque necessary to sustain steady disk rotation. They also showed that a stronger magnetic field depleted the disk surface thermal dispersion. Ariel [14] recently used asymptotic methods to study rotating disk flow under a magnetic field. These studies, however, considered the disk to be rigid, i.e., non-deformable.

Turkyilmazoglu [15] used a spectral numerical integration method to compute the steady-state hydromagnetic swirling flow from a radially stretchable spinning disk under a uniform axial magnetic field with viscous heating and wall suction. Bég *et al.* [16] extended the analysis in [15] to consider entropy generation minimization.

The above swirling disk flow studies did not consider nanoparticles or nanofluids. Nanofluids [17], of which magnetic nanopolymers [18] are a subset, are synthesized by suspending nanoparticles in base fluids. Nanoparticles may be metallic or carbon-based. The Tiwari-Das volume fraction model is a very popular model for simulating different nanoparticles [19]. Nanofluid dynamics from a rotating disk with or without magnetic fields have received substantial curiosity in current centuries in the fluid mechanics and manufacturing engineering communities. Humane *et al.* [20] discussed the thermo-solutal transport of magnetized Casson nanofluid doped with micro-organisms from a stretching sheet. Bég *et al.* [21] adopted a Chebyshev spectral collocation method (CSCM) to simulate the swirling Von-Karman convective flow through a resistant radially stretching disk in bioconvective nanofluid-saturated permeable media with anisotropic slip. Further studies of nanofluid transport in swirling Von Karman stream along a radially stretching disk have been presented by Umavathi and Bég [22, 23], who addressed copper oxide/titania/silver nanoparticles in aqueous base fluids.

The above studies only considered *unitary nanofluids* i. e. single-nanoparticle scenarios. Thus, in recent studies, technologists have increasingly used the combination of multiple nanoparticles in different working solvents. This is known as *hybridized nanofluids* [24] and has been shown to achieve yet more impressive viscosity, thermal conductivity and flow performance characteristics compared with unitary nanofluids. Salawu *et al.* [25] applied a Galerkin weighted residual scheme with one-third of Simpson's method and MAPLE quadrature to study the swirling ferromagnetic hybrid nanofluid flowing from a radially stretching disk with varying thermal-magnetic possessions. Lv *et al.* [26] used a Parametric Continuation method (PCM) to simulate the impact of axial magnetic field, thermal radiation and Hall current on the hybrid micro-organism doped nanoliquid flow from a spinning disk. Redouane et al. [27] conducted research on a hybrid nanofluid's induced free flowing convection move in heated trigonal enclosure with rotating cylindrical cavity has been examined. Adnan et al. [28] demonstrated the impact of AA7072 and AA7075 aluminum alloy nanomaterials with multiple physical flow conditions. Manjunatha et al. [29] revealed the impact of variable viscosity on the drift over the boundary layer of a liquid by hybrid nanofluid properties. The impacts of thermal and thermo-hydraulic were quantified in Kumar et al. [30]

revision of the hybrid nanofluid flow experimentally in a mini-channel heat sink. Many other investigations have been examined for a range of hybrid nanoparticle designs including Kumar *et al.* [31] (Manganese-Zinc-Iron oxide-nickel and copper-alumina-iron oxide in decane base fluid), Kiran Kumar and Shamshuddin [32] (SWCNTs-MWCNTs nanofluids), Prakash *et al.* [33] (titania-alumina-copper nanoparticles), Kumar *et al.* [34] (Titanium dioxide and Graphene oxide nanoparticles with ethylene-glycol working solvent), Al-Kouz *et al.* [35] (water-Fe_3O_4/CNT hybrid magnetic nanofluid), Kumar *et al.* [36] (Oldroyd-B model CNTs-based hybrid nanoparticles with Kerosene oil as a base liquid), Tripathi *et al.* [37] (hybrid biocompatible silver and gold nanoparticles in variable viscosity blood), Chu *et al.* [38] (spherical/platelet/cylindrical copper nanoparticles), Wasim *et al.* [39] (gold and Copper nanoparticles with shape effects), Chamkha and Rashad [40] (rotating vertical cone), Krishna *et al.* [41] (rotating mixed convective flow in plate geometry), Chamkha and Rashad [42] (nanofluid flow in a permeable cone), and Takhar et al. [43] (mixed convection flow in rotating vertical cone).

The above studies have generally neglected rheological, i.e., *non-Newtonian* characteristics of either unitary or hybrid nanofluids. Rheology, however, has been shown to play a significant role in magnetic nanofluids since the re-orientation characteristics of the magnetic nanoparticles are modified by the complex viscosity due to non-Newtonian behaviour [44]. This is particularly prominent in electroconductive nano-polymers where tumbling, coiling, shear-thinning, shear-thickening, yield stress (viscoplastic), microstructural and viscoelastic relaxation and retardation (memory) effects may rise [45]. Several experimental works have confirmed these phenomena [46-48]. Recent investigations on *unitary* nanofluids include Nasir *et al.* [49] utilized the Maxwell viscoelastic model to analyse reactive nanofluid transport from a stretching wall with heat radiation. Pattnaik *et al.* [50] employed the Eringen micropolar model to study dual stratified (thermal/solutal) chemo-magnetic nanofluid boundary film stream from an elongated plane in permeable media. Nasir *et al.* [51] investigated tangent-hyperbolic nanofluid transport with wall suction and mixed convective boundary conditions. This has also been used in several unitary nanofluid studies, including Uddin *et al.* [52] (who studied heat-generating nanofluid flow in porous media with the Buongiorno model), Rana *et al.* [53] (who examined nano-layer conductivity and nanoparticle diameter effects in power-law nano-magnetic coating flow from a perforated tilted substrate), El-Dabe *et al.* [54] (who studied radiative flux effects on power-law magneto-nanofluid swirling disk flow) and Li *et al.* [55] (who considered precipitation effects in power-law nanofluid deposition on a spinning disk). Relevant investigations comprise Prakash *et al.* [56] (on electro-osmotic alumina/titania

nanofluids from a revolving wall), Kumar *et al.* [57] (on Titanium dioxide and graphene oxide hybrid nanoparticles in ethylene-glycol working solvent from a vertically ascending or descending rotating disk) and Bhatti *et al.* [58] (on Ni-MgO/H_2O hybridized nanofluid Hiemenz stagnation flow from a plastic stretchable surface in permeable media).

In certain magnetic materials fabrication operations, in addition to the magnetic (Lorentz) body force effect, other phenomena may arise. These include magnetic induction, magnetic dipole, Hall current, ion slip, Maxwell displacement current, magnetic relaxation and Joule dissipation. The latter is particularly crucial in high-temperature operations and has been studied in a variety of manufacturing systems, including iron-rich glass microwire coating [59], magnetic polymer extrusion and deposition [60] and dielectric spraying operations [61]. Several researchers have scrutinized the influence of Joule heating on magnetohydrodynamic coating flows. Khan *et al.* [62] studied numerically the hydromagnetic wire coating with a viscoelastic Eyring–Powell fluid considering Joule heating effects with a Runge–Kutta 4th-order method. Prakash *et al.* [63] computed the ionic electro-conductive rheological nanofluid bio-coating stream with a tangent hyperbolic model from a bi-directional stretchable plate under mutual orthogonal magnetic and electrical fields with Joule heating. Further numerical investigations contain Khashi'ie *et al*. [64], Thirumalaisamy *et al.* [65], and Shamshuddin *et al.* [66].

The above-mentioned research survey shows that various studies focus on nanofluid and hybrid nanofluid models. The aim and novelty of the current research are to scrutinise swirl smart, functional nano-polymeric coating systems more closely; a formulation is offered for the thermal convection distribution characteristics in a magnetic hybrid power-law rheological nanofluid polymer flowing from a radially stretching rotating disk. A *non-Fourier* [67,68] thermal flux formulation is deployed to simulate heat relaxation impacts absent in the classical Fourier thermal conduction model. A detailed parametric study is conducted to examine the transport characteristics (radial, azimuthal, axial velocities, temperature, tangential and radial plate drag and temperature gradient) for both Copper (Cu**)**/Aluminium alloy (AA7075**)** nanoparticles. Validation with distinct cases taken from the published articles. The present study features several novelties, including the first combined model for *Copper (Cu**)** and Aluminium alloys (AA7075**)** nanoparticles with Sodium Alginate ($C_6H_9Na0_7$) base fluid, radial disk stretching and non-Fourier heat flux*. It constitutes a significant step forward in more comprehensive simulations of thermo-magnetic nano-polymer spin coating manufacture.

2. Mathematical model for thermo-magnetic nano-polymer swirl coating

The manufacturing problem under consideration comprises the steady flow and thermal distribution in an incompressible, power-law rheological hybrid nanofluid (Cu-AA7075 with $C_6H_9Na0_7$ base fluid) from a radially stretching spinning isothermal disk with low electrical conductivity. Electrical polarization is ignored at the disk surface as is magnetic induction. The swirling system is subjected to an axial (vertical) static magnetic field, $B=(0,0,B_0)$. The swirling flow produces axisymmetric convective heat exchange to the ambient surrounding fluid due to the difference in heat transfer coefficients. A cylindrical coordinate (r,Φ,z) system is adopted, as depicted in **Figure 1**. The fluid stream is caused by uniform rotation (Ω) and stretching (c) of the disk surface with velocity, $u=cr$ where c is a constant (> 0 for stretching and < 0 for contracting). Due to axisymmetric flow, variation in the tangential, Φ direction is ignored. The z direction is perpendicular to the disk and r is the coordinate in the radial direction. T_w is the disk surface temperature and T_∞ is ambient heat, where $T_w > T_\infty$. Extending the earlier studies [69-71], by incorporating nanofluid characteristics and non-Fourier heat flux radial stretching, the governing momentum and energy equations can be shown to assume the following forms:

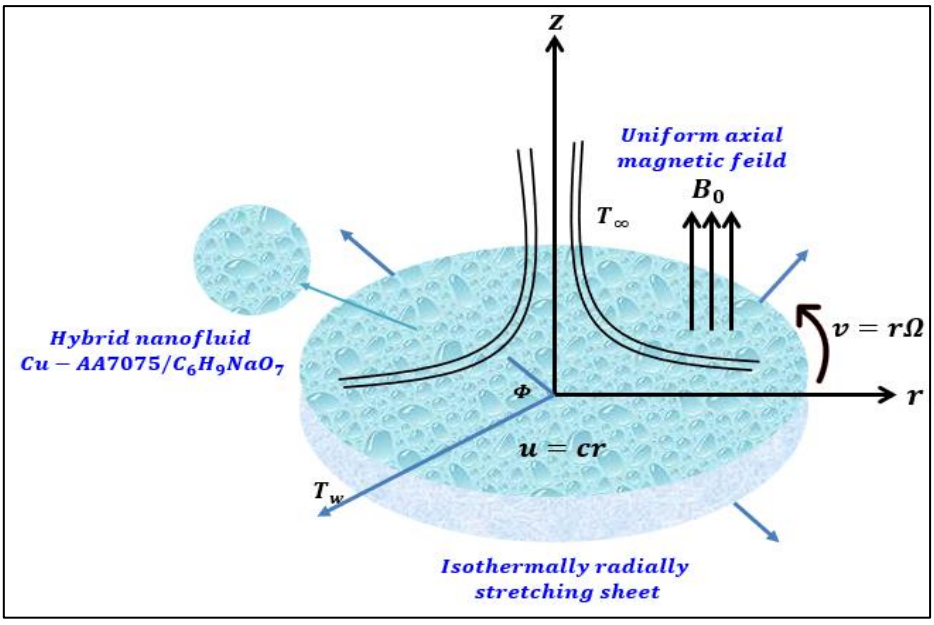

Fig 1: Magnetic hybrid nano-polymer swirl coating regime

$$\frac{\partial u}{\partial r}+\frac{u}{r}+\frac{\partial w}{\partial z}=0, \tag{1}$$

$$u\frac{\partial u}{\partial r}-\frac{v^2}{r}+w\frac{\partial u}{\partial z}=u_e\frac{du_e}{dr}+\frac{1}{\rho_{hnf}}\frac{\partial}{\partial z}\left(\mu\frac{\partial u}{\partial z}\right)-\left(\frac{\sigma_{hnf}B_0^2}{\rho_{hnf}}\right)(u-u_e), \tag{2}$$

$$u\frac{\partial v}{\partial r}+\frac{uv}{r}+w\frac{\partial v}{\partial z}=\frac{1}{\rho_{hnf}}\frac{\partial}{\partial z}\left(\mu\frac{\partial v}{\partial z}\right)-\left(\frac{\sigma_{hnf}B_0^2}{\rho_{hnf}}\right)v, \tag{3}$$

$$u\frac{\partial T}{\partial r}+w\frac{\partial T}{\partial z}+\lambda\left[u^2\frac{\partial^2 T}{\partial r^2}+w^2\frac{\partial^2 T}{\partial z^2}+2uw\frac{\partial^2 T}{\partial r\partial z}+\left(u\frac{\partial u}{\partial r}+w\frac{\partial u}{\partial z}\right)\frac{\partial T}{\partial r}+\left(u\frac{\partial w}{\partial r}+w\frac{\partial w}{\partial z}\right)\frac{\partial T}{\partial z}\right] = \frac{1}{\left(\rho c_p\right)_{hnf}}\left[\frac{\partial}{\partial z}\left(k\frac{\partial T}{\partial z}\right)\right], \quad (4)$$

Here (u,v,w) are flow rate modules in the (r,Φ,z) axes, T is temperature, u_e is free stream velocity, σ is electrical conductivity, ρ is density, c_p is specific heat capacity and λ is a non-Fourier parameter. Furthermore, μ and k designate the viscosity and heat conductivity based on the non-Newtonian power-law formulation are defined following Usman *et al*. [71] as:

$$\mu=\mu_{hnf}\left\{\left(\frac{\partial u}{\partial z}\right)^2+\left(\frac{\partial v}{\partial z}\right)^2\right\}^{(n-1)/2}, k=k_{hnf}\left\{\left(\frac{\partial u}{\partial z}\right)^2+\left(\frac{\partial v}{\partial z}\right)^2\right\}^{(n-1)/2}. \quad (5)$$

Here, n is the power-law rheological index ($n=1$ for Newtonian, $n<1$ for pseudoplastic and $n>1$ for dilatant nanofluids). The boundary constraints imposed on the disk wall and far stream are:

$$\left.\begin{aligned} &u=cr,\ \ v=\Omega r,\ \ w=0,\ \ k\frac{\partial T}{\partial z}=-h_1\left(T_w-T\right), \quad \text{at } z=0,\\ &u=u_e\to\delta r,\ \ v=v_e\to 0,\ \ w=0,\ \ T\to T_\infty, \qquad \text{at } z=\infty. \end{aligned}\right\}. \quad (6)$$

The effective properties of hybrid nanomaterial are defined follow as follows [72]:

Dynamic viscosity: $$\frac{\mu_{hnf}}{\mu_f}=\frac{1}{\left(1-\varphi_1\right)^{2.5}\left(1-\varphi_2\right)^{2.5}}=\frac{1}{A_1}, \quad (7)$$

Density: $$\frac{\rho_{hnf}}{\rho_f}=\left(1-\varphi_1\right)\left\{1-\varphi_1+\varphi_1\left(\frac{\rho_{s1}}{\rho_f}\right)\right\}+\varphi_2\left(\frac{\rho_{s2}}{\rho_f}\right)=A_2, \quad (8)$$

Electrical conductivity: $$\frac{\sigma_{hnf}}{\sigma_f}=1+\frac{3\left(\frac{\varphi_1\sigma_1+\varphi_2\sigma_2}{\sigma_f}-\left(\varphi_1+\varphi_2\right)\right)}{2+\left(\frac{\varphi_1\sigma_1+\varphi_2\sigma_2}{\left(\varphi_1+\varphi_2\right)\sigma_f}\right)-\left(\frac{\varphi_1\sigma_1+\varphi_2\sigma_2}{\sigma_f}-\left(\varphi_1+\varphi_2\right)\right)}=A_3, \quad (9)$$

Specific heat: $$\frac{\left(\rho c_p\right)_{hnf}}{\left(\rho c_p\right)_f}=\left(1-\varphi_2\right)\left\{1-\varphi_1+\varphi_1\left(\frac{\left(\rho c_p\right)_{s1}}{\left(\rho c_p\right)_f}\right)\right\}+\varphi_2\left(\frac{\left(\rho c_p\right)_{s2}}{\left(\rho c_p\right)_f}\right)=A_4, \quad (10)$$

Thermal conductivity:

$$\frac{k_{hnf}}{k_f} = A_5, where\ \frac{k_{hnf}}{k_f} = \frac{k_{s2} + 2k_{nf} - 2\varphi_2\left(k_{nf} - k_{s2}\right)}{k_{s2} + 2k_{nf} + 2\varphi_2\left(k_{nf} - k_{s2}\right)}\ and$$
$$\frac{k_{nf}}{k_f} = \frac{k_{s1} + 2k_f - 2\varphi_1\left(k_f - k_{s1}\right)}{k_{s1} + 2k_f + \varphi_1\left(k_f - k_{s1}\right)} \quad . \tag{11}$$

Here ϕ_1 and ϕ_2 symbolize the volume fraction nanoparticle of *Cu* and *AA*7075 respectively. The subscripts s_1, s_2, f, *nf* and *hnf* are used to represent the solid nanoparticle of *Cu*, the solid nanoparticle of *AA*7075, base fluid, nanomaterial and hybrid nanomaterial, correspondingly. Thermal, magnetic and other physical properties of *Cu* and *AA*7075 are offered in **Table 1**.

Table 1: Thermophysical characteristics of the base solvent and nanoparticles

Properties	Sodium Alginate ($C_6H_9Na0_7$) Ref. [72]	Copper (Cu) Ref. [73]	Aluminium alloys (AA7075) Ref. [74]
ρ [Kg/m^3]	989	8933	2810
C_p [J/Kg K]	4175	385.0	960
k [W/m K]	0.6376	400.0	173
σ [S/m]	0.00026	5.96x10^7	26.77x10^6

To render the conservation Eqns. (1)-(4) and boundary conditions (6) dimensionless, the following non-dimensional Von Karman transformations are invoked:

$$u = crF(\eta),\ v = crG(\eta),\ \eta = z\left(\frac{c^{2-n}}{\upsilon_f}\right)^{1/(n+1)} r^{(1-n)/(1+n)}$$
$$w = \left(\frac{c^{1-2n}}{\upsilon_f}\right)^{-1/(n+1)} r^{(n-1)/(n+1)} H(\eta),\ \theta(\eta) = \frac{T - T_\infty}{T_w - T_\infty}, \tag{12}$$

Incorporating the relations (7)-(11) and transformations (12) in Eqns. (1) – (4) yields a coupled nonlinear system of nonlinear ordinary derivative boundary layer equations in dimensionless form for axial, tangential and radial velocity and energy (heat):

$$H' = -2F - \frac{1-n}{1+n}\eta F', \tag{13}$$

$$F^2 - G^2 + \left(H + \frac{1-n}{1+n}\eta F\right)F' = \varepsilon^2 + \frac{A_2}{A_1}\left[F'\left\{\left(F'\right)^2 + \left(G'\right)^2\right\}^{(n-1)/2}\right]' - \frac{A_3}{A_1}M\left(F - \varepsilon\right), \tag{14}$$

$$2FG + \left(H + \frac{1-n}{1+n}\eta F\right)G' = \frac{A_2}{A_1}\left[G'\left\{\left(F'\right)^2 + \left(G'\right)^2\right\}^{(n-1)/2}\right]' - \frac{A_3}{A_1}MG, \tag{15}$$

$$\left[\beta\left\{\left(\frac{1-n}{1+n}\right)^2\eta^2+H^2+2\frac{1-n}{1+n}\eta FH\right\}\right]\theta''+\left[H+\frac{1-n}{1+n}\eta F+\beta\left\{2\frac{1-n}{1+n}FH\right\}\right]\theta'$$
$$+\beta\left[2\frac{1-n}{1+n}\right]=\frac{A_5}{A_4}\frac{1}{Pr}\left[\theta'\left\{\left(F'\right)^2+\left(G'\right)^2\right\}^{(n-1)/2}\right]', \tag{16}$$

The emerging dimensionless boundary conditions take the form:

$$\left.\begin{aligned}&F(0)=1,\ \ G(0)=\omega,\ \ H(0)=0,\ \ \theta(0)=1,\\&F(\infty)=\varepsilon,\qquad G(\infty)=0,\qquad \theta(\infty)=0.\end{aligned}\right\}. \tag{17}$$

In Eqns. (13)-(17) the following dimensionless parameters arise:

$$\left.\begin{aligned}&A_1=\frac{\rho_{hnf}}{\rho_f},A_2=\frac{\mu_{hnf}}{\mu_f},A_3=\frac{\sigma_{hnf}}{\sigma_f},A_4=\frac{\left(\rho c_f\right)_{hnf}}{\left(\rho c_f\right)_f},\ \ A_5=\frac{k_{hnf}}{k_f},\\&\varepsilon=\frac{\delta}{c},\ M=\frac{B_0^2\sigma}{\rho c},\ Pr=\frac{\nu}{\alpha},\ \beta=c\lambda,\ \omega=\frac{\Omega}{c}\end{aligned}\right\}. \tag{18}$$

Here A_1,A_2,A_3,A_4 are the hybrid nanofluid parameters. Also $M,\beta,\mathrm{Pr},\omega$ and ε denote the magnetic body force term, thermal non-Fourier relaxation term, Prandtl number, rotation term and flow rate ratio parameter (due to radial stretching of the disk). Several wall characteristics are critical in materials processing operations. These are the gradients of the velocity components and temperature i.e., *tangential and radial disk friction (wall shear stress modules) and Nusselt number*, and are described as follows:

$$C_{Fr}=\frac{\tau_{rz}}{\rho_f(cr)^2},\ C_{G\phi}=\frac{\tau_{\phi z}}{\rho_f(cr)^2},\ Nu_r=\frac{r\,q_w}{k(T_w-T_\infty)}. \tag{19}$$

Here:

$$\left.\begin{aligned}&\tau_{rz}=\left[\mu\left\{\left(\frac{\partial u}{\partial z}\right)+\frac{1}{r}\left(\frac{\partial w}{\partial\phi}\right)\right\}\right]_{z=0}=\left[\mu\left(\frac{\partial u}{\partial z}\right)\right]_{z=0},\\&\tau_{\theta^* z}=\left[\mu\left\{\left(\frac{\partial v}{\partial z}\right)+\frac{1}{r}\left(\frac{\partial w}{\partial\phi}\right)\right\}\right]_{z=0}=\left[\mu\left(\frac{\partial v}{\partial z}\right)\right]_{z=0},\\&q_w=\left[-k\frac{\partial T}{\partial z}+\left(q_r\right)_w\right]_{z=0}=-\left[k\frac{\partial T}{\partial z}\right]_{z=0}\end{aligned}\right\}, \tag{20}$$

The required dimensionless forms are:

$$\left.\begin{aligned}&\mathrm{Re}_r^{1/(n+1)}\,C_{Fr}=\left[F'^2(0)+G'^2(0)\right]^{(n-1)/2}F'(0),\\&\mathrm{Re}_r^{1/(n+1)}\,C_{G\phi}=\left[F'^2(0)+G'^2(0)\right]^{(n-1)/2}G'(0),\\&\mathrm{Re}_r^{-1/(n+1)}\,Nu_r=-\left[1+Rd\left(1+(\theta_w-1)\theta(0)\right)^3\right]\theta'(0),\end{aligned}\right\} \tag{21}$$

Here, the radial local Reynolds number is represented as $\mathrm{Re}_r = r^2 c^{2-n} / \nu_f$.

3. Numerical Solution

The non-dimensional boundary problem described by Eqns. (13)-(16) under constraints (17) model is strongly coupled and nonlinear. Analytical solutions are inflexible. A numerical approach is thus deployed. A weighted residual scheme (WRS) with an integrating Galerkin method [75] is utilized due to excellent versatility, convergence, stability and consistency features. The characteristics of the used techniques made it more reliable and preferable than other solution methods. This approach is equally adept at accommodating linear and nonlinear derivative equations and complex boundary constraints. The solution procedure adopts trial functions for *tangential velocity (G), axial velocity (H), radial velocity (F), and temperature (*θ*)* following [75,76] in the form:

$$F(\eta) = \sum_{i=0}^{r} a_i e^{-\frac{\eta i}{2}},\ G(\eta) = \sum_{i=0}^{r} b_i e^{-\frac{\eta i}{2}},\ H(\eta) = \sum_{i=0}^{r} c_i e^{-\frac{\eta i}{2}},\ \theta(\eta) = \sum_{i=0}^{r} d_i e^{-\frac{\eta i}{2}} \quad (22)$$

Here a_i, b_i, c_i and d_i are constant coefficients to be determined, $e^{-\frac{\eta i}{2}}$ defines the weighting function adopted to satisfy the flow boundary conditions, r is a secure number which takes $r = 0,1,2,3, \dots, N-2$. Therefore, imposing the base functions (22) on the equations (13-16) to have the residual system of equations, R_F, R_G, R_H and R_θ in terms of a's, b's, c's, and d's. Also, the trial functions are used on the boundary conditions (17) to obtain a system of linear equations. Thus, the residual errors are minimized as much as possible to zero using an approximation integrating the Galerkin method with the following definitions for residuals:

$$\int_0^L R_F e^{-\frac{\eta i}{2}} d\eta = 0,\ \int_0^L R_G e^{-\frac{\eta i}{2}} d\eta = 0,\ \int_0^L R_H e^{-\frac{\eta i}{2}} d\eta = 0,\ \int_0^L R_\theta e^{-\frac{\eta i}{2}} d\eta = 0 \quad (23)$$

The minimization of residual errors is achieved by taking the integral and weighting function product of $e^{-\frac{\eta i}{2}}$ and the residual equations. The numerical solution is executed in MAPLE symbolic software in which platform the WRM-Galerkin procedure has been coded. The procedure is repeated to study the effects of different control parameters in the swirling hybrid nanofluid model.

4. Validation

To verify the correctness of the extant numerical methodology, **Table 2** compares the radial velocity gradient solution, $F'(0)$, obtained with the present WRM-Galerkin solutions *in the absence of magnetic, non-Fourier thermal relaxation, rotation and radial stretching effects* i.

e. $M = \varepsilon = \beta = \omega = 0$, with the earlier computations of Anders *et al.* [77], Ming *et al.* [78] and Usman *et al.* [71]. Excellent agreement is obtained for the case of Prandtl number *Pr =1* and a range of power-law rheological index values (n = 0.5 to 1.3). This confirms the validity of the present WRM-Galerkin code, which is demonstrably suitable for multi-physical boundary layer flows.

Table 2: Results verification for $F'(0)$ with different values of the power-law index (n) when $Pr = 1, M = \varepsilon = \beta = \omega = 0$.

n	Anders *et al.* [77]	Ming *et al.* [78]	Usman *et al.* [71]	Present WRM-Galerkin solutions
0.5	0.501	0.50058	0.5006	0.50057833
0.8	0.504	0.50381	0.5038	0.50380648
1.0	0.510	0.51021	0.5102	0.51021455
1.3	0.522	0.52150	0.5215	0.52150496
1.5	0.529	0.52919	0.5292	0.52918529

5. Results and Discussion

In this section, we investigate the effect of selected terms on the swirling boundary layer magnetic hybrid rheological nanofluid flow (containing hybridized Copper (Cu**)** and Aluminum alloy (AA7075**)** nanoparticles with Sodium Alginate ($C_6H_9Na0_7$) as base fluid) over the rotating stretching disk. **Figs. 1- 10** Visualize the graphical solutions for (axial velocity (H), tangential velocity (G), radial velocity (F) and temperature (θ)). **Table 3** documents the radial and tangential plate friction components and energy gradient solutions. In all cases, default data has been prescribed carefully to correlate with actual magnetic nano-polymers [60].

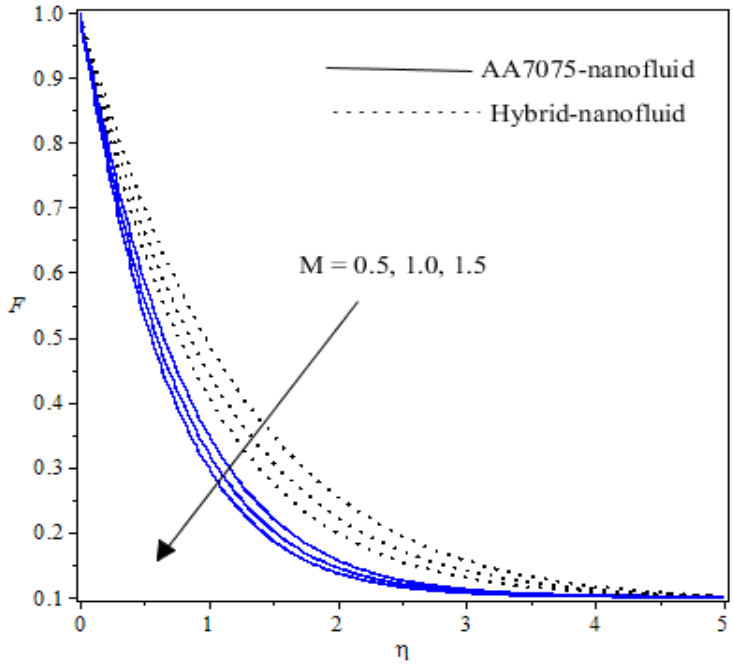

Fig 2. Profile of radial velocity component for various values of magnetic term, M

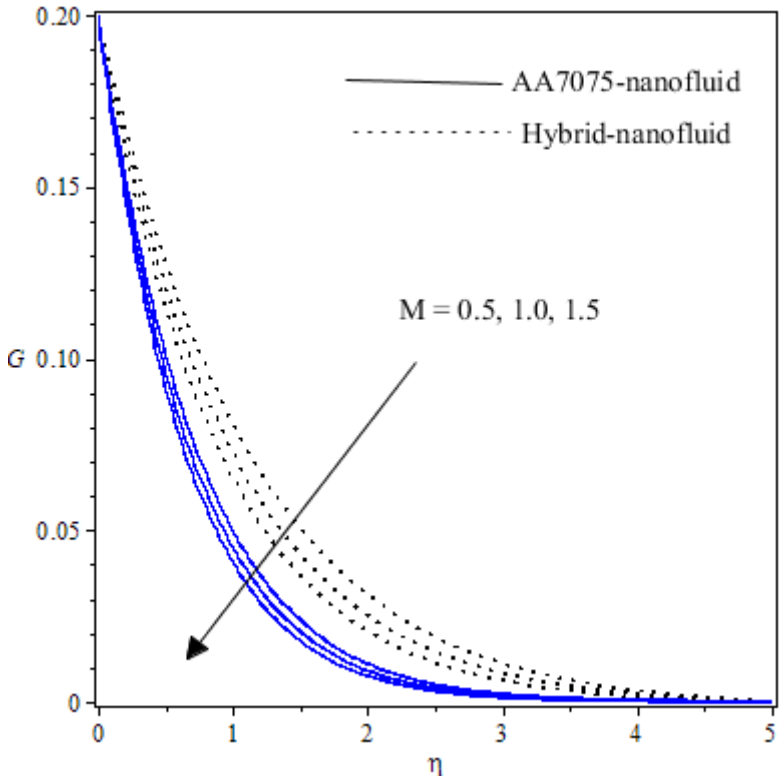

Fig 3. Profile of tangential velocity for various values of magnetic term, M

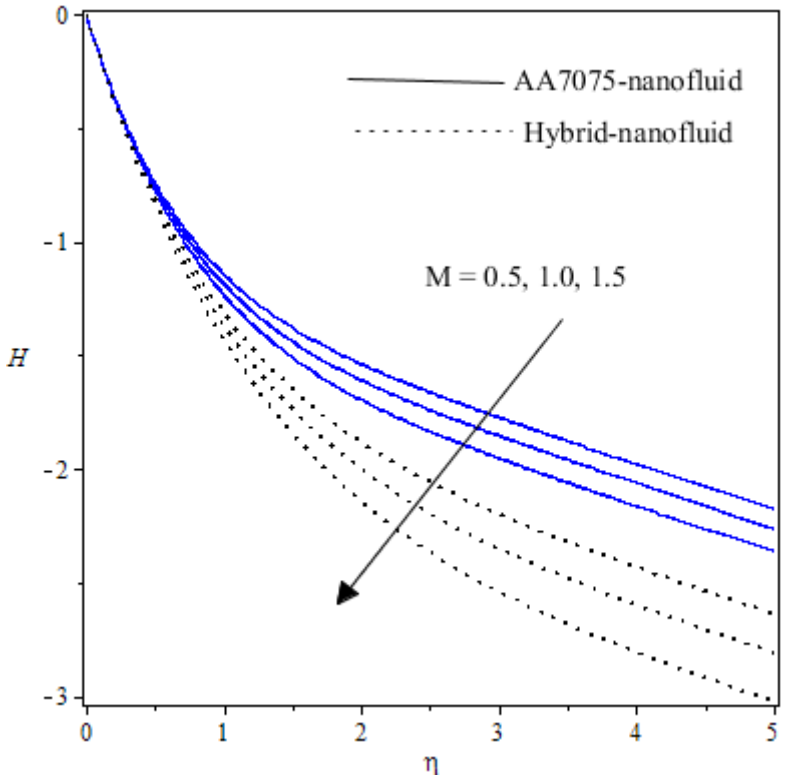

Fig 4. Profile of axial velocity component for various values of magnetic term, M

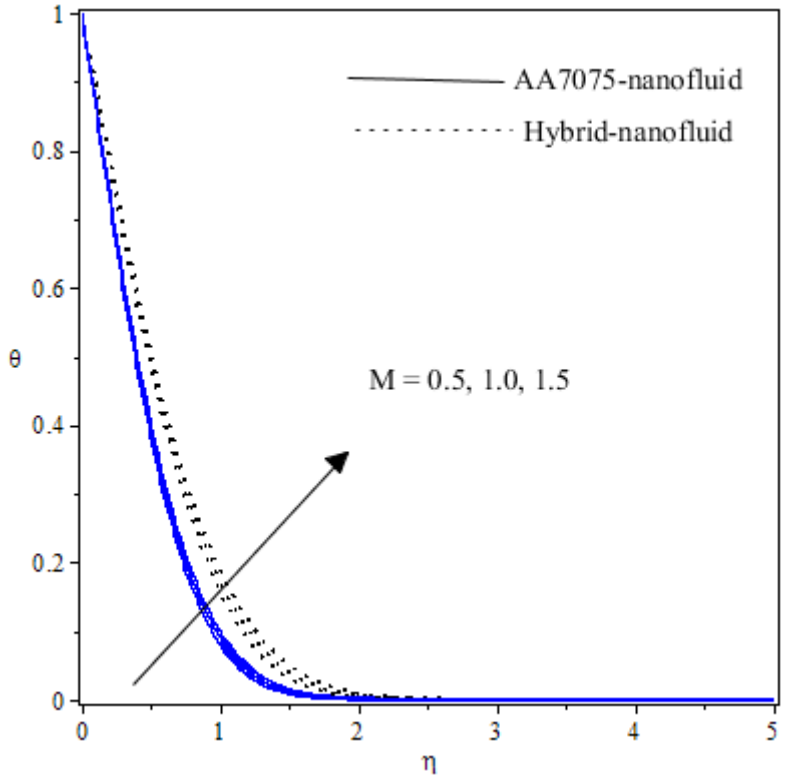

Fig 5. Profile of temperature with different values of magnetic term, M

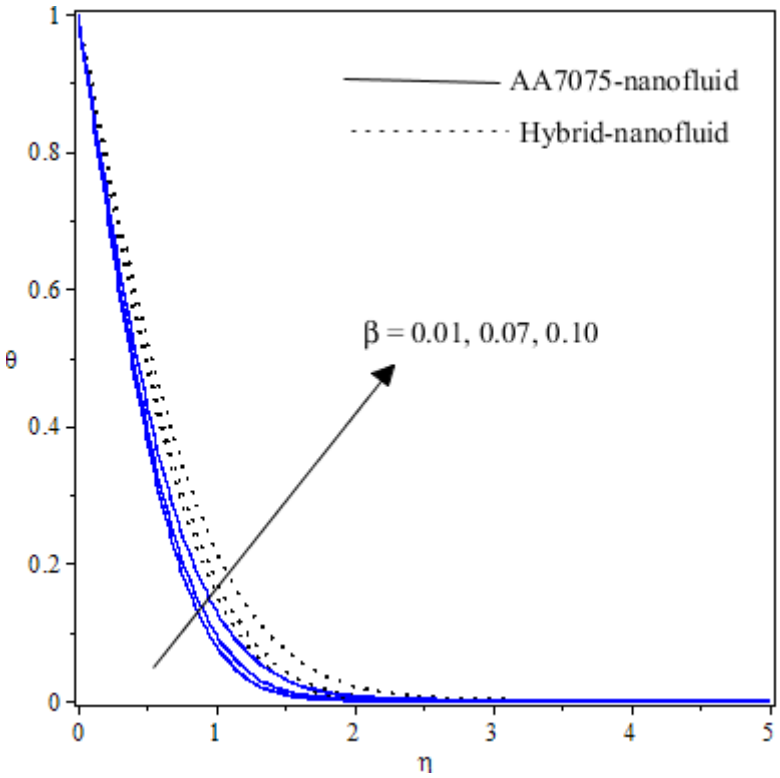

Fig 6. Profile of temperature with various values of thermal relaxation parameter values, β

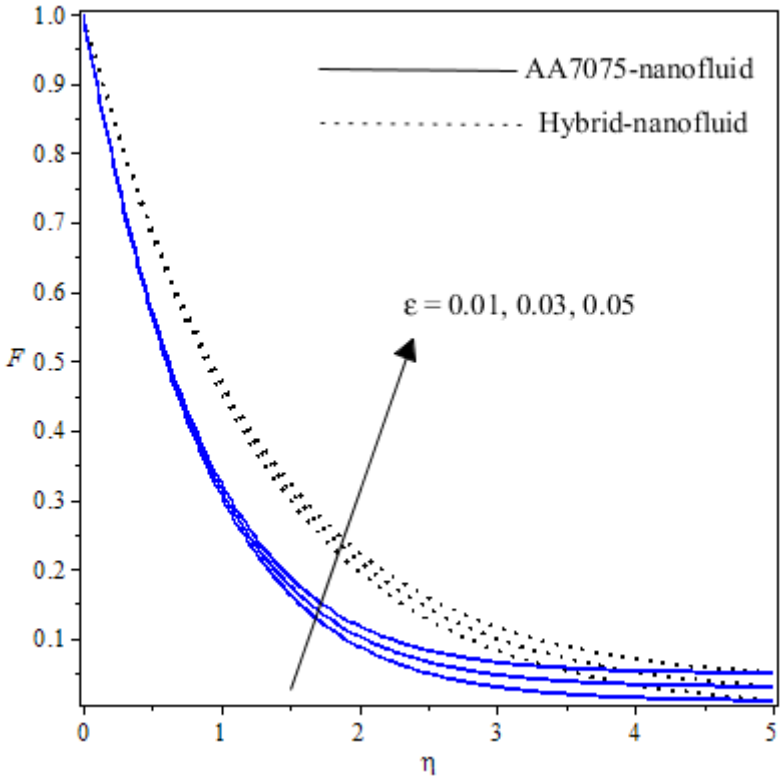

Fig 7. Profile of radial velocity with various velocity ratio parameter values, ε

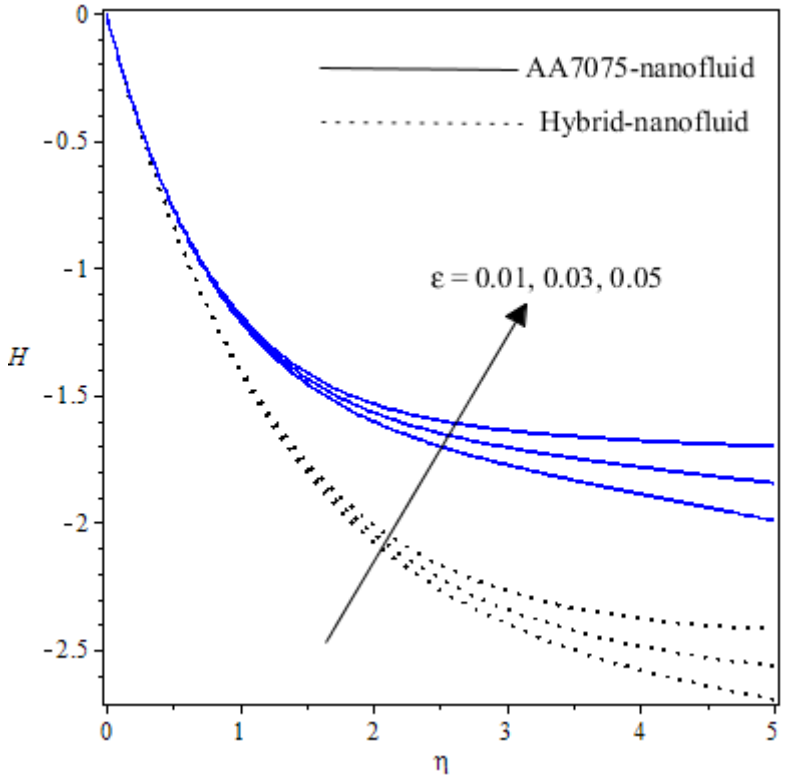

Fig 8. Evolution in axial velocity profiles with various values of velocity ratio parameter ε

Figs 2- 4 illustrate the axial, radial and tangential velocities response to a change in magnetic field. The magnetic field appears in the radial and tangential momenta equations since its axial orientation (*z*-direction) is mutually orthogonal to the radial and tangential directions. The Lorentz body force components are, therefore, generated in both the radial (14) and tangential directions (15) and take the forms, $-\frac{A_3}{A_1}M(F-\varepsilon)$ and $-\frac{A_3}{A_1}MG$, respectively. The Lorentz force is absent in the axial momentum eqn. (13). Increasing M values induces A significant damping effect in both the radial and tangential flow fields (Figs 2, 3). The axial flow is also decelerated (Fig 4) with increments in magnetic parameter; however, values are consistently negative.

Fig. 5 visualizes the temperature evolution through the boundary film region oblique to the disk plate with a change in magnetic field parameter, M . In all cases, there is a sharp descent from the disk surface in temperature, which then decays smoothly to the free stream. Higher M values produce a strong elevation in temperature values.

Fig. 6 depicts the distribution in temperature with various values of heat relaxation term values, β. In the absence of thermal relaxation, $\beta = 0$ and the energy eqn. (16) contracts to $[H + \frac{1-n}{1+n}\eta F]\theta' = \frac{A_5}{A_4}\frac{1}{Pr}\left[\theta'\{(F')^2 + (G')^2\}^{\frac{(n-1)}{2}}\right]'$ which corresponds to the classical Fourier model.

The non-Fourier model substantially modifies the heat flux terms and introduces hyperbolic finite wave conduction effects known as thermal relaxation. The classical Fourier model negates this effect and is a parabolic model. With increasing β values, there exists high augmentation in temperatures computed.

Figs. 7 and 8 exemplify the evolution in radial and axial velocity with various radial velocity stretching term values ε. This term ascends in the free stream boundary condition for radial velocity i. e. Eqn. (17), $F(\infty) = \varepsilon$. As noted earlier, we consider the case of radial stretching, for which $\varepsilon > 0$. A strong momentum boost is imparted to the radial flow with greater values of this parameter (Fig. 7). The radial stretching corresponds to deformable disk behaviour, which can be used in spin coating to manipulate the coating characteristics further. The reverse axial flow is reduced, and lesser negative values are computed in axial velocity at higher values of ε (Fig. 8). Overall, stronger radial stretching manifests in a boost in both radial and axial momentum. Again, higher (less negative) axial velocities are computed for hybrid copper (Cu**)-**aluminium alloy (AA7075**)-**sodium alginate ($C_6H_9Na0_7$) nanofluid. at all axial coordinate, η, relative to the unitary AA7075 nanofluid.

Supplementary Fig. 9 displays the distribution of tangential velocity (G) for various rotational parameter values, ω. The rotational parameter, $\omega = \Omega / c$ features in the disk surface (wall) tangential velocity boundary condition (17), $G(0) = \omega$. It relates the relative contribution of disk rotational velocity to the intensity of the radial stretching velocity. When $\omega = 1$ both rotation and stretching contribute equally. For $\omega < 1$, the stretching dominates. However, the contribution from the Coriolis rotating body force produces a strong accentuation in tangential (swirl) momentum. This enhances tangential velocity substantially, specifically in the vicinity of the disk plate and near it. Further from the disk wall towards the free stream, the effect is diminished.

Supplementary Figs. 10-13 depict the impact of variation in the power-law index values on the flow characteristic evolutions. The power-law index signifies Newtonian fluid when $n = 1$, pseudoplastic nanofluid when $n < 1$ and dilatant nanofluid when $n > 1$. As presented in **Supplementary Figs 10, 11 and 13**, increasing values of *n* for aluminium alloy (AA7075**)-**sodium alginate ($C_6H_9Na0_7$) and $Cu - AA7075/C_6H_9Na0_7$ hybrid nanofluid decreases the radial and axial tangential velocity components. Velocity magnitudes are minimized for the Newtonian case (n =1). However, in all cases, they are maximum for the strongly pseudo-plastic case (n = 0.5) since the shear-thinning properties (lower global viscosity) encourage momentum diffusion, accelerating the flow. Clearly, the use of a Newtonian model under-

predicts the velocity characteristics, leading to erroneous estimates for the actual behaviour of the hybrid nanofluids. In **Supplementary Fig 12,** the temperature of strongly pseudoplastic nanofluid (n = 0.5) is also shown to exceed that of Newtonian nanofluid (n =1). The shear-thinning nature of the nanofluid, as noted earlier, reduces viscosity. The smaller the value of n, the more prominent the pseudoplastic behaviour. Thermal convection is, therefore, exacerbated in the swirling boundary layer, and temperatures are boosted as n is reduced. Thermal boundary layer thickness will also, therefore, be increased. The Newtonian model (n = 10) under-predicts temperatures and thermal boundary layer thickness. Therefore, the justification for including a rheological model is evident as it is more appropriate for nano-polymers.

Supplementary Table 3 presents the effects of all five control parameters on radial skin friction, tangential skin friction and Nusselt number, for $\mathrm{Cu}-\mathrm{AA7075}/\mathrm{C_6H_9Na0_7}$ hybrid nanofluid. There is no tangible modification in either the radial ($Re_r^{\frac{1}{n+1}}C_{Fr}$) or the tangential ($Re_r^{\frac{1}{n+1}}C_{G\phi}$) skin friction with increasing non-Fourier parameter, β. However, the heat transferred to the disk surface is reduced since temperatures are enormously elevated with non-Fourier heat flux. Nusselt number is therefore depleted. With increasing rotation parameter, ω, radial skin friction is decreased whereas tangential skin friction is elevated. Stronger rotation also generates a weak rise in Nusselt number (heat transfer rate at the disk), implying cooling in the boundary layer. With elevation in magnetic parameter, M, both radial and skin friction magnitudes are increased whereas Nusselt number is decreased. Elevation in velocity ratio parameter, ε, reduces radial skin friction but enhances tangential (azimuthal) skin friction and Nusselt number. Finally, an increment in the Prandtl number, is observed to not influence radial and tangential skin friction but strongly elevates the Nusselt number since the boundary layer is cooled and there is an exacerbation in heat (thermal energy) transferred to the disk surface.

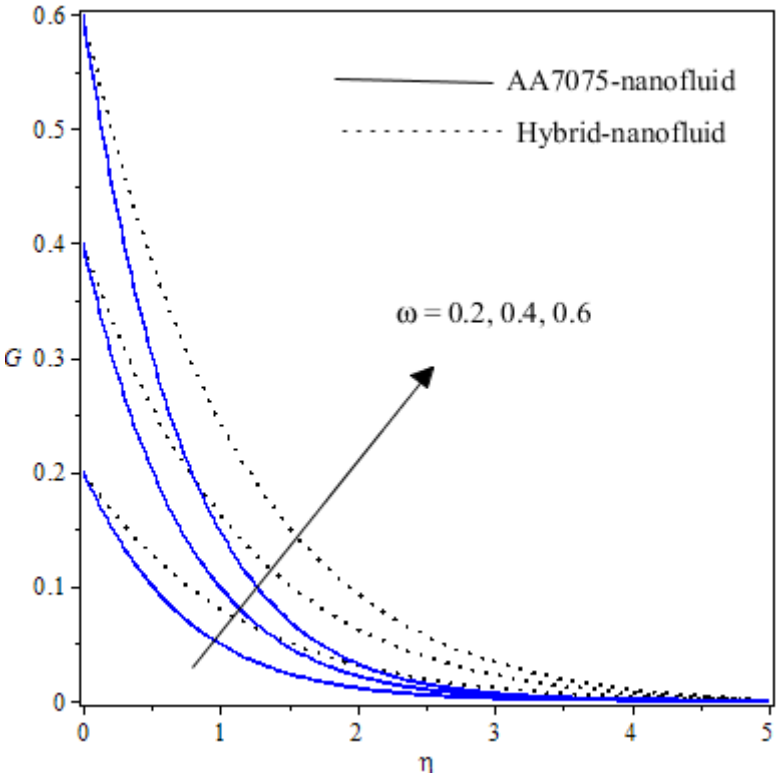

Supplementary Fig 9. Distribution of tangential velocity for various rotational parameter values, ω

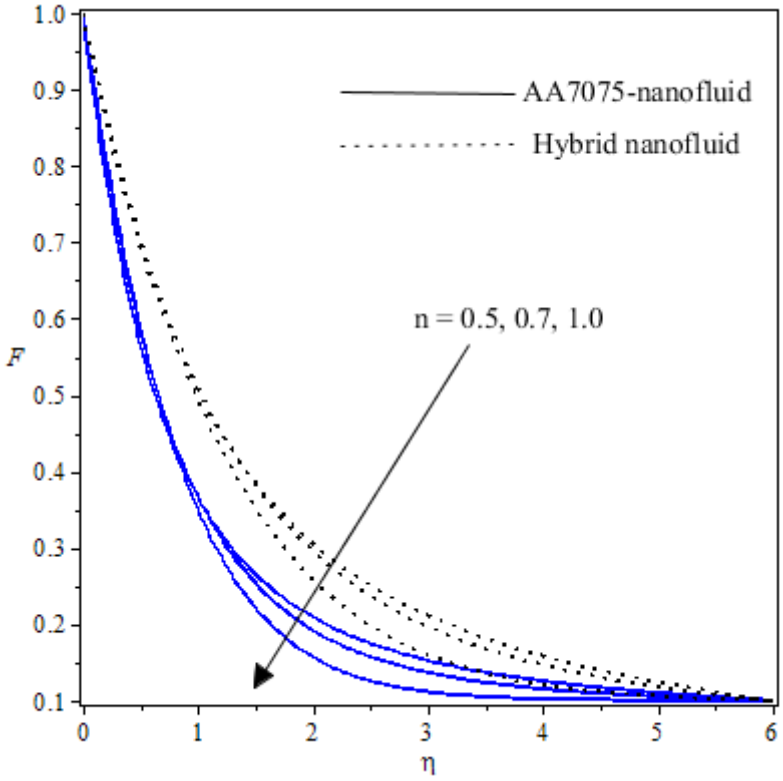

Supplementary Fig 10. Radial velocity field for various power-law index, n

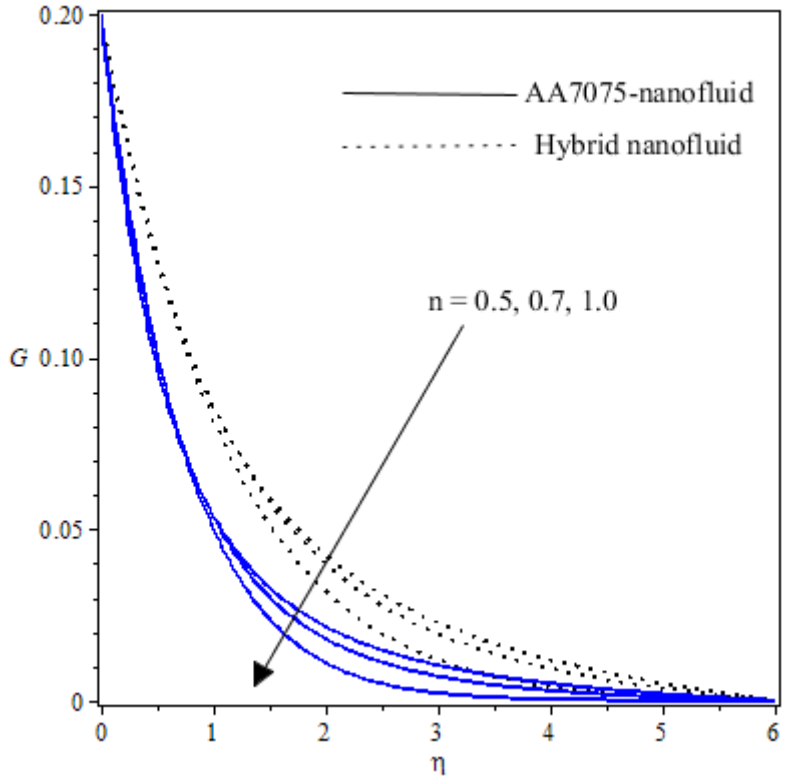

Supplementary Fig 11. Evolution of axial velocity field for diverse power-law index, n

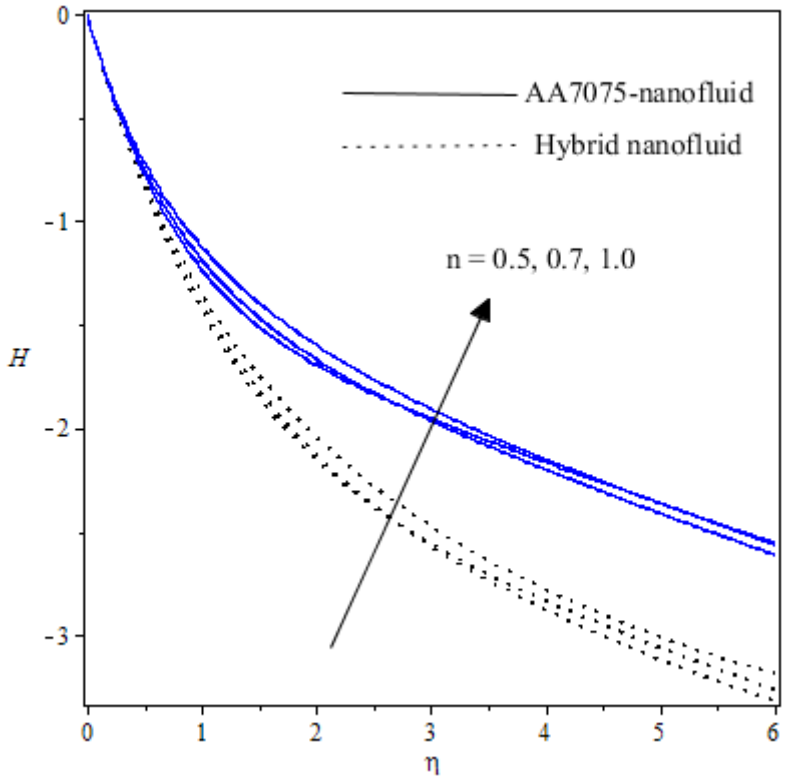

Supplementary Fig 12. Tangential velocity distribution for diverse power-law index, n

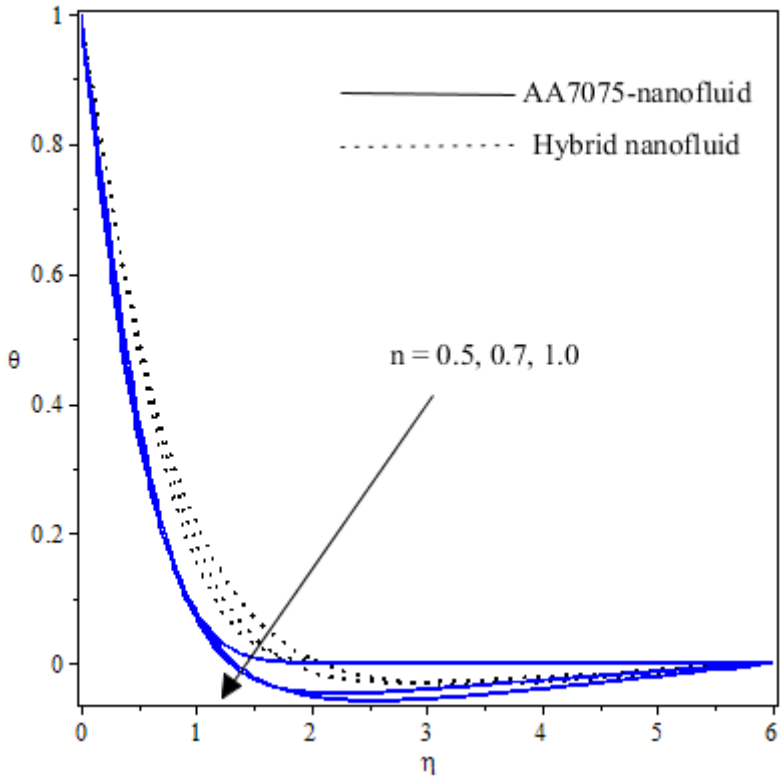

Supplementary Fig 13. Temperature evolution profile for varying power-law index, n

Supplementary Table 3: Computed values for the hybridized $Cu - AA7075/C_6H_9Na0_7$ nanofluid

β	ω	M	ε	Pr	$Re_r^{\frac{1}{n+1}}C_{Fr}$	$Re_r^{\frac{1}{n+1}}C_{G\phi^*}$	$Re_r^{\frac{1}{n+1}}Nu_r$
0.10	0.2	0.5	0.10	3	-0.701204104	-0.175628522	1.130683467
0.05					-0.701204105	-0.175628522	1.074738776
	0.4				-0.689753295	-0.351682951	1.132925710
	0.6				-0.670741709	-0.528578265	1.136623785
		1.0			-0.820074549	-0.199304562	1.099739207
		2.0			-1.018848058	-0.240222898	1.049972223
			0.03		-0.736838593	-0.173751846	1.116068355
			0.07		-0.716867849	-0.174819389	1.124361165
				1.0	-	-	0.573229979
				2.0	-	-	0.886323851

6. Conclusions

As a simulation of thermo-magnetic nano-polymer spin coating manufacture, a theoretical and computational study has been presented for convective heat transfer in magnetic hybrid power-

law rheological nanofluid polymer flowing from a stretching rotating disk. copper (Cu**)** and aluminium alloys (AA7075**)** nanoparticles with sodium alginate ($C_6H_9Na0_7$) as base fluid are considered, and a hybrid volume fraction model is deployed. A *non-Fourier* (Cattaneo-Christov) heat flux model has been implemented to simulate thermal relaxation effects absent in the classical Fourier heat conduction model. Using appropriate similarity variables with the Von Karman transformations, the system of governing conservation partial differential equations with associated boundary conditions has been reduced to an ordinary differential boundary value problem. This boundary value problem has been solved computationally with the weighted residual method (WRM) and an integral Galerkin scheme, executed in the MATLAB symbolic software. A detailed parametric study has been conducted to examine the transport characteristics (radial, azimuthal, axial velocities, temperature, radial and tangential skin friction and Nusselt number) for both copper (Cu**)**/aluminium alloy (AA7075**)** nanoparticles. Verification of the accuracy of the solutions with exceptional cases from the literature has been included. The principal findings of the present computations can be summarized as follows:

- An increase in magnetic parameter, *M*, strongly damps the radial, tangential and axial velocity but substantially elevates temperature and thermal boundary layer thickness.
- Hybrid copper (Cu**)**-aluminum alloy (AA7075)-sodium alginate (C6H9Na07) nanofluid attains markedly greater temperatures than AA7075 unitary nanofluid at all locations into the boundary layer.
- With increasing non-Fourier relaxation parameter values, there is a strong increment in temperature and thermal boundary layer thickness, whereas the Nusselt number is diminished. Temperatures are shown to be under-predicted by the classical Fourier model ($\beta = 0$).
- With elevation in velocity stretching ratio parameter, ε, radial velocity is enhanced and reverse axial flow is damped. However, radial skin friction is suppressed, and tangential (azimuthal) skin friction and Nusselt number are both increased.
- With greater rotational parameter, ωA strong acceleration is induced in the tangential flow, and the Nusselt number is weakly incremented, whereas radial skin friction is suppressed.
- With an increment in the power-law rheological index (n), axial, tangential, and radial velocity magnitudes are reduced, as are temperature and thermal boundary layer thickness. Strongly pseudoplastic nano-polymers (lower *n* value) achieve greater velocity and temperature magnitudes relative to Newtonian nanofluids.

Future studies may consider the Buongiorno two-component nanoscale model, which includes nanoparticle mass diffusion, and additionally explore a non-Fickian model. Also, alternative non-Newtonian models, including viscoelastic and microstructural models, can be investigated. Efforts in these directions will be communicated imminently, and the Weighted Residual Method (WRM) and Galerkin numerical approach hold significant promise.

Conflicts of Interest

None to declare.

References

[1] Bannwarth, M. B., S. Utech., S. Ebert., D. A. Weitz., D. Crespy., and K. Landfester. "Colloidal polymers with controlled sequence and branching constructed from magnetic field assembled nanoparticles." *ACS Nano* 9 (2015):2720– 2728.

[2] Li, Y., Q. Liu., A. J. Hess., S. Mi., X. Liu., Z. Chen., Y. Xie., and I. I. Smalyukh. "Programmable ultralight magnets via orientational arrangement of ferromagnetic nanoparticles within aerogel hosts." *ACS Nano* 13 (2019):13875– 13883.

[3] Ma, M., Q. Zhang., J. Dou., H. Zhang., D. Yin., W. Geng., and Y. Zhou. "Fabrication of one-dimensional Fe3O4/P(GMA–DVB) nanochains by magnetic-field-induced precipitation polymerization." *Journal of Colloid Interface Science* 374 (2012): 339– 344.

[4] Adam, A. A., J. O. Dennis., Y. Al-Hadeethi., E. M. Mkawi., B. A. Abdulkadir., F. Usman., Y. M. Hassan., I. A. Wadi., and M. Sani. "State of the art and new directions on electrospun lignin/cellulose nanofibers for supercapacitor application: a systematic literature review." *Polymers* 12 (2020):2884. https://doi.org/10.3390/polym12122884

[5] Hadipour, A., and M. E. Bharololoom. "Influence of type of bath agitation (magnetic stirring and rotating disk cathode) on tribological properties of nickel electrodeposits." *Protection of Metals and Physical Chemistry of Surfaces* 54 (2018): 274–281.

[6] Mazurek, A., and M. Trzaska. "The influence of the bath stirring on the structure and properties of Ni/diamond composite coatings produced electrochemically." *Inynieria Powierzchni* 25 (2020):14–19.

[7] Zhou, P. W., and Y. B. Zhong. "Behaviour of Fe/nano-Si particles composite electrodeposition with a vertical electrode system in a static parallel magnetic field." *Electrochimica Acta* 111 (2013):126-135.

[8] Koza, J. A., M. Uhlemann., C. Mickel., A. Gebert., and L. Schultz. "The effect of magnetic field on the electrodeposition of CoFe alloys." *Journal of Magnetism and Magnetic Materials* 321(2009): 2265–2268.

[9] Tang, L., J. J. Kang., P. F. He., S. Ding., S. Chen., M. Liu., Y. Xiong., G. Ma., and H. Wang. "Effects of spraying conditions on the microstructure and properties of NiCrBSi coatings prepared by internal rotating plasma spraying." *Surface Coating Technology* 374 (2019): 625-633.

[10] Gupta, R. N., and A. K. Das. "Pulse electrocodeposited Ni–WC composite coating." *Materials and Manufacturing Processes* 31 (2016): 42–47.

[11] Kármán, T. V. "Uber laminare und turbulente reibung." *Zeitschrift Fur Angewandte Mathematik und Physik* 1(4) (1921):233-252.

[12] Cochran, W. G. “The flow due to a rotating disk.” *Proceedings- Cambridge Philosophy Society* 30 (1934):365-375.
[13] Sparrow, E. M., and R.D. Cess. “Magnetohydrodynamic flow and heat transfer about a rotating disk. *ASME Journal of Applied Mechanics* 29 (1962):181-187.
[14] Ariel, P. D. “On computation of MHD flow near a rotating disk.” *Zeitschrift Fur Angewandte Mathematik und Physik* 82(4) (2002):235-246.
[15] Turkyilmazoglu, M. “MHD fluid flow and heat transfer due to a stretching rotating disk.” *International Journal of Thermal Science* 51 (2012):195-201.
[16] Anwar Bég, O., M. M. Rashidi., and N. F. Mehr. “Second law analysis of hydromagnetic flow from a stretching rotating disk: DTM-Padé simulation of novel nuclear MHD propulsion systems.” *Frontiers in Aerospace Engineering* 2(1) (2013): 29-38.
[17] Das, S. K., S. U. S. Choi., W. Yu., and T. Pradeep. “Nanofluids: Science and Technology.” John Wiley and Sons, New York (2007).
[18] Vekas, L. “Magnetic nanofluids properties and some applications.” *Journal of Physics* 49 (2004): 707-721.
[19] Tiwari, R. K., and M. K. Das, “Heat transfer augmentation in a two-sided lid-driven differentially heated square cavity utilizing nanofluids.” *International Journal of Heat and Mass Transfer* 50 (2007): 2002-2018.
[20] Humane, P. P., V. S. Patil., MD. Shamshuddin., G. R. Rajput., and A. B. Patil. “Role of bioconvection on the dynamics of chemically active Casson nanofluid flowing via an inclined porous stretching sheet with convective conditions.” *International Journal of Modelling and Simulations* (2022). https://doi.org/10.1080/02286203.2022.2164156.
[21] O. Anwar Bég, M. N. Kabir., M. J. Uddin., A. I. M. Ismail., and Y. Alginahi. “Numerical investigation of Von Karman swirling bioconvective nanofluid transport from a rotating disk in a porous medium with Stefan blowing and anisotropic slip effects.” *Proceedings of IMechE- Part C- Journal of Mechanical Engineering Science* 235 (2020): 3933-3951.
[22] Umavathi, J. C., and O. Anwar Bég. “Computation of Von Karman thermo-solutal swirling flow of a nanofluid over a rotating disk to a non-Darcian porous medium with hydrodynamic/thermal slip.” *Journal of Thermal Analysis and Calorimetry* 147(2021):8445-8460.
[23] Umavathi, J. C., O. Anwar Bég., T. A. Bég., and A. Kadir. “Swirling bioconvective nanofluid flow from a spinning stretchable disk in a permeable medium.” *International Journal of Modelling and Simulations* (2022). https://doi.org/10.1080/02286203.2022.2122928.
[24] Kshirsagar, D. P., and M. Venkatesh. “A review on hybrid nanofluids for engineering applications.” *Materials Today Proceedings* 44 (2020):744–755.
[25] Salawu, S. O., MD. Shamshuddin., and O. Anwar Bég. “Influence of magnetization, variable viscosity and thermal conductivity on Von Karman swirling flow of H_2O-Fe_3O_4 and H_2O-Mn-$ZNFe_2O_4$ ferromagnetic nanofluids from a stretchable rotating disk: smart spin coating simulation.” *Material Science and Engineering B* 279 (2022): 115659. https://doi.org/10.1016/j.mseb.2022.115659
[26] Lv, Y. P., E. A. Algehyne., M. G. Alshehri., E. Alzahrani., M. Bilal., M. A. Khan., and M. Shuaib. “Numerical approach towards gyrotactic micro-organisms hybrid nanoliquid flow with the Hall current and magnetic field over a spinning disk.” *Scientific Reports*11(1) (2021):1–13.
[27] Redouane, F., W. Jamshed., S. S. U. Devi., M. Prakash., N. A. A. M. Nasir., Z. Hammouch., M. R. Eid., K. S. Nisar., A. B. Mahammed., A. H. A. Aty., I. S. Yahia., E. M. Eed. “Heat flow saturate of Ag/MgO-water hybrid nanofluid in heated trigonal enclosure with rotate cylindrical cavity by using Galerkin finite element.” *Scientific Reports* 12 (2022): 2303. https://doi.org/10.1038/s41598-022-06134-6

[28] Adnan., S. I. U. Khan., U. Khan., N. Ahmed., S. T. Mohyud-Din., I. Khan., K. S. Nisar. "Thermal transport investigation in AA7072 and AA7075 aluminum alloys nanomaterials based radiative nanofluids by considering the multiple physical flow conditions." *Scientific Reports* 11 (2021): 9837. https://doi.org/10.1038/s41598-021-87900-w

[29] Manjunatha, S., B. A. Kuttan., S. Jayanthi., A. J. Chamkha., B. J. Gireesha. "Heat transfer enhancement in the boundary layer flow of hybrid nanofluids due to variable viscosity and natural convection." *Heliyon* 5(4) (2019): e01469. https://doi.org/10.1016/j.heliyon.2019.e01469

[30] Kumar, V., S. Kr. Singh., V. Kumar., W. Jamshed., K. S. Nisar. "Thermal and thermo-hydraulic behavior of alumina-graphene hybrid nanofluid in mini-channel heat sink: An experimental study." *International Journal of Energy Research* 45(15) (2021): 20700-20714. https://doi.org/10.1002/er.7134

[31] Kumar, R. N., R. P. Gowda., A. M. Abusorrah., Y. M. Mahrous., N. H. Abu-Hamdeh., A. Issakhov., and B. C. Prasannakumara. "Impact of magnetic dipole on ferromagnetic hybrid nanofluid flow over a stretching cylinder." *Physica Scripta* 96(4) (2021): 045215. https://doi.org/10.1088/1402-4896/abe324

[32] Kiran Kumar, T., and MD. Shamshuddin. "Thermal Performance on radiative and Ohmic dissipative magneto-nanoliquid over moving flat plate suspended by SWCNTs and MWCNTs." *Journal of Nanofluids* 12 (2023): 192-201. https://doi.org/10.1166/jon.2023.1945.

[33] Prakash, J., D. Tripathi., O. Anwar Bég. "Comparative study of hybrid nanofluid performance in microchannel slip flow induced by electroosmosis and peristalsis." *Applied Nanoscience* 10 (2020):1693-1706.

[34] Kumar, R. N., R. J. Gowda., B. J. Gireesha., and B. C. Prasannakumara. "Non-Newtonian hybrid nanofluid flow over vertically upward/downward moving rotating disk in a Darcy-Forchheimer porous medium." *European Physical Journal: Special Topics* 230(5) (2021):1227–1237.

[35] Al-Kouz, W., A. Abderrahmane., MD. Shamshuddin., O. Younis., S. Mohammed., O. Anwar Bég., D. Toghraie. "Heat transfer and entropy generation analysis of water-Fe_3O_4/CNT hybrid magnetic nanofluid flow in a trapezoidal wavy enclosure containing porous media with the Galerkin finite element method." *European Physical Journal Plus*136 (2021): 1184.https://doi.org/10.1140/epjp/ s13360-021-02192-3

[36] Shahzad, F., W. Jamshed, M. R. Eid, R. W. Ibrahim, R. Safdar, K. S. Nisar, and MD. Shamshuddin. "Thermal amelioration in heat transfer using Oldroyd-B model hybrid nanofluid by CNTs-based kerosene oil flow in solar collector applications." *Waves in Random and Complex Media* (2022). https://doi.org/10.1080/17455030.2022.2157511.

[37] Tripathi, J., B. Vasu., O. Anwar Bég., R. S. R. Gorla. "Unsteady hybrid nanoparticle-mediated magneto-hemo-dynamics and heat transfer through an overlapped stenotic artery: biomedical drug delivery simulation." *Proceedings of IMechE. Part H – Journal of Engineering Medicine* 235(10) (2021):1175-1196. https://doi.org/10.1177/09544119211026095.

[38] Chu, Y. M., U. Nazir., M. Sohail., M. M. Selim., and J. R. Lee. "Enhancement in thermal energy and solute particles using hybrid nanoparticles by engaging activation energy and chemical reaction over a parabolic surface via finite element approach." *Fractal and Fractional* 5(3) (2021):119. https://doi.org/10.3390/fractalfract5030119.

[39] Wasim, J., M. R. Eid., F. Shahzad., R. Safdar., and MD. Shamshuddin. "Keller box analysis for thermal efficiency of magneto time-dependent nanofluid flowing in solar-powered tractor applications applying nano-metal shaped factor." *Waves in Random and Complex Media* (2022). https://doi.org/10.1080/17455030.2022.2146779.

[40] Chamkha, A. J., A. M. Rashad. "Unsteady heat and mass transfer by MHD mixed convection flow from a rotating vertical cone with chemical reaction and Soret and Dufour effects." *The Canadian Journal of Chemical Engineering* 92(4) (2014): 758-767.

[41] Krishna, M. V., B. V. Swarnalathamma., A. J. Chamkha. "Investigations of Soret, Joule and Hall effects on MHD rotating mixed convective flow past an infinite vertical porous plate." *Journal of Ocean Engineering and Science* 4(3) (2019): 263-275.

[42] Chamkha, A. J., A. M. Rashad. "Natural convection from a vertical permeable cone in a nanofluid saturated porous media for uniform heat and nanoparticles volume fraction fluxes." *International Journal of Numerical Methods for Heat and Fluid Flow* 22(8) (2012) 1073-1085.

[43] Takhar, H. S., A. J. Chamkha., G. Nath. "Unsteady mixed convection flow from a rotating vertical cone with a magnetic field." *Heat and Mass Transfer* 39 (2003): 297–304. https://doi.org/10.1007/s00231-002-0400-1

[44] Mostarac, D., and S. S. Kantorovich. "Rheology of a nano-polymer synthesized through directional assembly of DNA nanochambers for magnetic applications." *Macromolecules* 55(15) (2022): 6462–6473.

[45] Katiyar, A., A. N. Singh., P. Shukla., and T. Nandi. "Rheological behaviour of magnetic nanofluids containing spherical nanoparticles of Fe–Ni." *Powder Technology* 224 (2012): 86-89.

[46] Qiao, X., M. Bai., K. Tao., X. Gong., R. Gu., H. Watababe., K. Sun., J. Wu., and X. Kang. "Magneto rheological behaviour of polythene glycol-coated Fe_3O_4 ferrofluids." *Journal of the Society of Rheology* 38 (2009): 23-30.

[47] Hong, R. Y., Z. Q. Ren., Y. P. Han., H. Z. Li., Y. Zhang., and J. Ding. "Rheological properties of water based Fe_3O_4." *Chemical Engineering Science* 62 (2007): 5912-5924.

[48] Rosenfeld, N., N. M. Wereley., R. Radhakrishnan., and T. S. Sudarshan., "Behaviour of magneto-rheological fluids utilizing nanopowder iron." *International Journal of Modern Physics B* 16 (2022): 2392-2398.

[49] Nasir, M., M. Waqas., O. Anwar Bég., M. Zamri., and H. J. Leonard. "Chemically reactive Maxwell nanoliquid flow from a stretching surface with Newtonian heating, nonlinear convection and radiative flux: nanopolymer flow processing simulation." *Nanotechnology Reviews* 11 (2022):1291–1306.

[50] Pattnaik, P. K., M. M. Bhatti, S. R. Mishra, M. A. Abbas, and O. Anwar Bég, "Mixed convective-radiative magnetized micropolar nanofluid flow over a stretching surface in porous media with double stratification and chemical reaction effects: ADM-Padé computation." *Journal of Mathematics* 2022 (2022): 9888379. https://doi.org/ 10.1155/2022/9888379.

[51] Nasir, M., M. Waqas., O. Anwar Bég., M. Zamri., H. J. Leonard., and K. Guedri. "Dynamics of tangent-hyperbolic nanoliquids configured by stratified extending surface: Effects of transpiration, Robin conditions and dual stratifications." *International Communications in Heat and Mass Transfer* 139 (2022): 106372. https://doi.org/10.1016/j.icheatmasstransfer.2022.106372

[52] Uddin, M. J., N. H. M. Yusoff., O. Anwar Beg., and A. I. M. Ismail. "Lie group analysis and numerical solutions for non-Newtonian nanofluid flow in a porous medium with internal heat generation.' *Physica Scripta* 87 (2013): 025401. https://doi.org/10.1088/0031-8949/02/025401.

[53] Rana, P., and O. Anwar Bég. Mixed convection flow along an inclined permeable plate: effect of magnetic field, nanolayer conductivity and nanoparticle diameter. *Applied Nanoscience* 5 (2015): 569-581.

[54] EL-Dabe, N. T., A. A. Hazim., M. A. I. Essawy., I. H. Abd-elmaksoud., A. A. Ramadan, and A. H. Abdel-Hamid. "Non-linear heat and mass transfer in a thermal radiated MHD flow of a power-law nanofluid over a rotating disk." *SN Applied Science* 1 (2019): 551. https://doi.org/10.1007/s42452-019-0557-6.

[55] Li, B., X. Chen., L. Zheng., J. Zhu., and T. Wang. "Precipitation phenomenon of nanoparticles in power-law fluids over a rotating disk." *Microfluidics and Nanofluidics* 17 (2014):107-114.

[56] Prakash, J., D. Tripathi., O. Anwar Bég., A. K. Tiwari., and R. Kumar. "Thermo-electro kinetic rotating non-Newtonian hybrid nanofluid flow from an accelerating vertical surface." *Heat Transfer* 51(2) (2022): 1746-1777.

[57] Kumar, R. N., R. J. P. Gowda., B. J. Gireesha., and B. C. Prasannakumara. "Non-Newtonian hybrid nanofluid flow over vertically upward/downward moving rotating disk in a Darcy–Forchheimer porous medium." *The European Physical Journal: Special Topics* 230 (2021):1227–1237.

[58] Bhatti, M. M., O. Anwar Bég., and S. I. Abdelsalam. "A computational framework of magnetized MgO-Ni/Water based hybrid nanofluid stagnation flow on an elastic stretching surface through a porous medium with application in solar energy coatings." *Nanomaterials* 12(7) (2022):1049. https://doi.org/10.3390/nano12071049.

[59] Gonzalez, A., V. Zhukova., M. Ipatov., P. Corte-Leon., J. M. Blanco., and A. Zhukova. "Effect of Joule heating on GMI and magnetic properties of Fe-rich glass-coated microwires." *AIP Advances* 12 (2022): 03502. https://doi.org/ 10.1063/9.0000290

[60] Fiorillo, F., G. Bertotti., C. Appino., and M. Pasquale. "Soft Magnetic Materials." In: Webster J., editor. Wiley Encyclopaedia of Electrical and Electronics Engineering, John Wiley & Sons, Inc.; Torino, Italy (1999).

[61] Niittymaki, M., K. Lahti., T. Suhonen, and J. Metsajoki. "Effect of temperature and humidity on dielectric properties of thermally sprayed alumina coatings." *IEEE Transactions in Dielectrics and Electrical Insulation* 25 (2018): 908–918.

[62] Khan, Z., H. U. Rasheed., T. Abbas., W. Khan., I. Khan., D. Baleanu., K. S. Nisar. "Analysis of Eyring-Powell fluid flow used as a coating material for wire with variable viscosity effect along with thermal radiation and Joule heating." *Crystals* 10(3) (2020):168.https://doi.org/10.3390/cryst10030168.

[63] Prakash, J., D. Tripathi., A. Nevzat., and O. Anwar Bég. "Tangent hyperbolic non-Newtonian radiative bioconvection nanofluid flow from a bi-directional stretching surface with electro-magneto-hydrodynamic, Joule heating and modified diffusion effects." *European Physical Journal Plus* 137 (2022): 472. https://doi.org/10.1140/epjp/s13360-022-02613-x.

[64] Khashi'ie, N. S., N. M. Arifin., I. Pop., and N. S. Wahid. "Flow and heat transfer of hybrid nanofluid over a permeable shrinking cylinder with Joule heating: A comparative analysis." *Alexandria Engineering Journal* 59 (2020): 1787-1798.

[65] Thirumalaisamy, K., R. Sivaraj., V. R. Prasad., O. Anwar Bég., H. H. Leung., F. Kamalov., and K. Vajravelu. "Comparative heat transfer analysis of γAl_2O_3 and γ-Al_2O_3-$C_2H_6O_2$ electroconductive nanofluids in a saturated porous square cavity with Joule dissipation and heat source/sink effects." *Physics of Fluids* 34 (2022): 072001. https://doi.org/ 10.1063/5.0095334.

[66] Hussain, A., M. Y. Malik., T. Salahuddin., S. Bilal., and M. Awais. "Combined effects of viscous dissipation and Joule heating on MHD Sisko nanofluid over a stretching cylinder." *Journal of Molecular Liquids* 231 (2017): 341-352.

[67] Shamshuddin, MD., F. Shahzad., J. Wasim., O. Anwar Beg., M. R. Eid., and T. A. Beg. "Thermo-solutal stratification and chemical reaction effects ion radiative magnetized

nanofluid flow along an exponentially stretching sensor plate: Computational analysis." *Journal of Magnetism and Magnetic Materials* 565 (2023):170286. https://doi.org/10.1016/j.jmmm.2022.170286

[68] Imtiaz, M., F. Shahid., T. Hayat., and A. Alsaedi. "Chemical reactive flow of Jeffrey fluid due to a rotating disk with non-Fourier heat flux theory." *Journal of Thermal Analysis and Calorimetry* 140 (2020): 2461–2470.

[69] Ming, C., L. Zheng., and X. Zhang. "Steady flow and heat transfer of the power-law fluid over a rotating disk." *International Communication in Heat and Mass Transfer* 38 (2011): 280-284.

[70] Ming, C., L. Zheng., X. Zhang., F. Liu., and V. Anh. "Flow and heat transfer of power-law fluid over a rotating disk with generalized diffusion." *International Communication in Heat and Mass Transfer* 79 (2016):81-88.

[71] Usman., P. Lin., A. Ghaffari., and I. Mustafa. "A theoretical analysis of steady three-dimensional flow and heat transfer of power-Law nanofluid over a stretchable rotating disk filled with gyrotactic microorganism." *Physica Scripta* 96 (2021): 015008. https://doi.org/10.1088/1402-4896/abc647

[72] Hussanan, A., M. Qasim., and Z. M. Chen. "Heat transfer enhancement in sodium alginate based magnetic and non-magnetic nanoparticles mixture hybrid nanofluid." *Physica A: Statistical Mechanics and Applications* 550 (2020): 123957. https://doi.org/10.1016/j.physa.2019.123957.

[73] Gholinia, M., S. Gholinia., Kh. Hosseinzadeh., and D. D. Ganji. "Investigation on ethylene glycol Nano fluid flow over a vertical permeable circular cylinder under effect of magnetic field." *Results in Physics* 9 (2018): 1525-1533.

[74] Waqas, H., S. A. Khan., and T. Muhammad. "Thermal analysis of magnetized flow of AA7072-AA7075/blood-based hybrid nanofluids in a rotating channel." *Alexandria Engineering Journal* 61(4) (2022): 3059-3068.

[75] Salawu, S. O., H. A. Ogunseye., MD. Shamshuddin., and A. B. Disu. "Reaction-diffusion of double exothermic couple stress fluid and thermal criticality with Reynolds viscosity and optical radiation." *Chemical Physics* 561 (2022):111601. https://doi.org/10.1016/j.chemphys.2022.111601.

[76] Hassan, A. R., S. O. Salawu., A. B. Disu., and O. R. Aderele. "Thermodynamic analysis of a tangent hyperbolic hydromagnetic heat generating fluid in quadratic Boussinesq approximation." *Journal of Computational Mathematics and Data Science* 4 (2022):100058. https://doi.org/10.1016/j.jcmds.2022.100058.

[77] Anders, H. I., E. De Korte., and R. Meland. "Flow of a power-law fluid over a rotating disk revisited." *Fluid Dynamics Research* 28 (2011):75–88.

[78] Ming, C. Y., L. Zheng., and X. Zhang. "Steady flow and heat transfer of the power-law fluid over a rotating disk." *International Communication in Heat and Mass Transfer* 38 (2011): 280-284.